Polarity of ultrathin MgO(111) films deposited on a metal substrate

Jacek Goniakowski,[1,2] Livia Giordano,[3] and Claudine Noguera[1,2]
[1]*Institut des Nanosciences de Paris, CNRS, UMR 7588, 140 rue de Lourmel, 75015 Paris, France*
[2]*INSP, UPMC-Univ. Paris 6, UMR 7588, 140 rue de Lourmel, 75015 Paris, France*
[3]*Dipartimento di Scienza dei Materiali, Università di Milano–Bicocca, Via R. Cozzi, 53, 20125 Milano, Italy*
(Received 18 February 2010; revised manuscript received 8 April 2010; published 3 May 2010)

We present a theoretical density-functional theory study of the effect of deposition on a metal substrate (Mg, Pt, Ag, and Au) on the phase diagram of ultrathin MgO(111) polar films. By considering various crystallographic structures (rocksalt, zinc-blende, and graphiticlike), layer stackings and lattice registries at the interface, we identify the two principal mechanisms by which oxide films interact with the metal substrate. On one hand, metal provides the charges necessary for polarity compensation at the interface, enables the oxide ions at the interface to recover their usual valence, and induces a strong stabilization of polar films. On the other hand, due to interfacial bonding and band alignment (function of the metal electronegativity), a second type of electron exchange occurs at the interface, dominant in films which are either nonpolar or uncompensated polar. It induces a structural distortion of the oxide film in the interface region and yields a nonvanishing film polarization. The stabilizing effect of the metal substrate is considerably weaker in this case.

DOI: 10.1103/PhysRevB.81.205404 PACS number(s): 68.55.−a, 64.70.Nd, 81.30.Dz

I. INTRODUCTION

The last decade has witnessed important advances in the fabrication and characterization of crystalline ultrathin oxide films supported on metals. It has rapidly become clear that the rich variety of their unusual and tailored structures as well as their specific electronic properties may noticeably modify the substrate reactivity[1–6] and may control nucleation sites, shape, and reactivity of supported metal atoms or clusters.[7,8] For example, it has been shown that the change of work function induced by the oxide layer[9–14] induces a spontaneous charging of metal adsorbates,[15–17] and, in some cases, may lead to adsorbate self-organization.[18–21]

More specifically, ultrathin oxide films of polar orientations have attracted interest due, in particular, to a successful growth of well-controlled crystalline MgO(111) films and islands, such as those on Ag(111),[22–25] Mo(110),[26] and Au(111),[27] substrates. Moreover, on more general basis, it has been pointed out that contrary to what happens at polar surfaces of bulk oxides, polarity at the nanoscale may be at the origin of a vast spectrum of novel effects and could be used as an additional lever for tuning material properties.[28,29] Indeed, on bulk oxide surfaces, polarity (divergent total dipole moment) requires an electrostatic compensation which is achieved by an adequate modification of the surface charge density.[30,31] Conversely, at the nanoscale, since the total dipole moment always remains finite, it may be simply sustained by the oxide film, producing an uncompensated polar state with strongly thickness-dependent properties.[29] In other cases, ultrathin films may heal polarity by a thorough structural transformation, leading to novel "surface oxides," with no bulk counterparts.[28]

While the above scenarios apply to unsupported polar oxide films, realistic predictions must include the effect of the metal substrate. The latter is expected to be particularly important since the stabilizing role of a metal/oxide interface at polar surfaces of bulk oxides has already been demonstrated.[32,33] On the other hand, the existence of a strong electrostatic coupling between the interface charge transfer and the atomic structure of an oxide *monolayer* has been reported.[34] It has been shown that a structural distortion (rumpling) appears in the oxide film, creating a dipole moment which opposes and partially compensates that due to the interfacial charge transfer.

In this context, the aim of the present paper is to systematically incorporate the effect of a metal substrate in the understanding of polarity-related effects in oxide thin films as a function their thickness. To this goal we reconsider the generic case of an ionic insulator (MgO) and we simulate (1×1)-MgO(111) epitaxial ultrathin films [1–4-monolayer (ML) thick] on surfaces of a variety of metals ranging from simple (Mg), to transition (Pt), and noble (Ag, Au). We consider three crystallographic structures of the oxide film: rocksalt (B1), zinc-blende (B3), and graphiticlike h-BN (B_k), which correspond to qualitatively different polarity characteristics in unsupported films.[28,29] Indeed, rocksalt MgO(111) films require charge compensation; at the smallest thicknesses, they are unstable and relax spontaneously to the zinc-blende structure. Zinc-blende films display a peculiar noncompensated polar state, in which the total dipole moment is sustained by the oxide films without any modification of the surface charge density. Graphiticlike films are the most stable due to the planar configuration of the Mg_3O_3 rings and the resulting nonpolar character of the (0001) surface.

The paper is organized as follows. Section II presents the details of the computational setup. Sections III–V are devoted to a detailed analysis of the MgO(111)/Pt(111) case: structural phase diagram, polarity characteristics, and total dipole moment. On these grounds, trends along the series of four metals are established in Sec. VI and conclusions are given in Sec. VII.

II. METHODOLOGY

The calculations rely on the density-functional theory at the PW-91 gradient-corrected level[35] with the projector aug-

mented wave method[36] and a plane-wave-basis set (kinetic energy cutoff of 400 eV), as implemented in VASP.[37] All MgO/metal systems are modeled by asymmetric five-layer-thick metal slabs with one bare surface and one surface covered with the MgO film, separated by a vacuum layer of at least 10 Å. The spurious interaction between the dipoles of the neighboring supercells is eliminated by means of the so-called dipole correction. All structures are fully relaxed until the residual forces are less than 0.01 eV/Å. Atomic charges are estimated within a Bader method.[38,39]

As in our previous study on metal-supported oxide monolayers,[34] we use structural models which focus on the effect of metal-oxide bonding at the interface and on the characteristics of the metal substrate as electron reservoir, rather than on lattice mismatch considerations. We work with (1×1) unit cells at the equilibrium lattice parameter of *supported* oxide films and the metal substrates are distorted accordingly. The equilibrium lattice parameters of the supported films are estimated from the minimum of the total energy difference between MgO/metal and metal subsystems. Such procedure eliminates the first-order contribution due to the metal distortion and minimizes essentially the energy of the oxide film augmented by the interaction energy at the metal/oxide interface.

In addition to stoichiometric films, characterized by an equal number of oxygen and magnesium atomic layers, we have considered also nonstoichiometric ones. Within the (1×1) cells, these latter are characterized by one excess atomic layer of either oxygen or magnesium, and can be considered as representative for oxygen- or magnesium-rich objects obtained from layer-by-layer growth/oxidation experiments.

III. MgO/Pt(111): STRUCTURAL PHASES, STACKING, AND REGISTRY

We start with a description of the properties of 1–4-ML-thick MgO films supported on a Pt(111) substrate. We consider the effect of stacking (oxygen or magnesium layer at the interface), of local lattice registry (oxygen or magnesium on-top of metal atoms), and of film stoichiometry. A comparison with the results obtained for unsupported films enables a quantification of the stabilizing role of the Pt(111) substrate.

Figure 1 gives the structural phase diagrams for Pt(111) supported and unsupported 1–4-ML-thick MgO ultrathin films. The most stable stacking sequence (oxygen at the interface) and interface registry (oxygen on-top of Pt atoms) are used in the stoichiometric films. Figure 1 displays also the results obtained for nonstoichiometric films in the rocksalt structure. In the unsupported case, nonstoichiometry has a strong stabilizing effect on films in this bulklike structure, shifting their formation energies close to those of the alternative structures.[40] Moreover, contrary to their stoichiometric counterparts, the thinnest unsupported nonstoichiometric rocksalt films do not transform spontaneously into the zinc-blende ones. Finally, because of their charge-compensated polar character, an additional strong stabilizing effect by the metal substrate is expected. The two types of nonstoichiometric films (O or Mg rich) are characterized by different

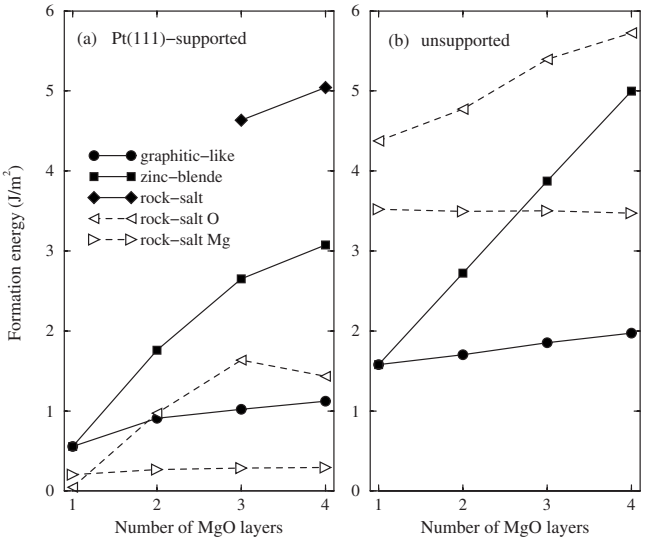

FIG. 1. Structural phase diagram of (a) Pt(111)-supported and (b) self-standing MgO films in graphiticlike, zinc-blende, and rocksalt structures. Formation energies (J/m^2) are calculated with respect to bulk (rocksalt) MgO with an additional reference to half an oxygen molecule or to bulk magnesium for, respectively, nonstoichiometric oxygen-rich (rocksalt O) and magnesium-rich (rocksalt Mg) films.

stacking sequences, respectively, oxygen (oxygen on-top metal registry) or magnesium at the interface (magnesium on-top metal registry). In order to calculate the formation energies, we used a reference to, half an oxygen molecule (oxygen-rich conditions) or bulk magnesium (magnesium-rich conditions).

Comparison of the two panels in Fig. 1 shows that the phase diagram is globally unchanged in the presence of the metal substrate. In stoichiometric films, the graphiticlike structure remains the most stable one and the rocksalt the most unstable. However, in all cases, the metal substrate stabilizes the MgO films. This is particularly clear for the 3–4-ML stoichiometric rocksalt films which relax to the zinc-blende structure when unsupported but exist in a metastable state when deposited on the Pt(111) substrate. Lowering of formation energy is very large for nonstoichiometric rocksalt films (on the order of 4 J/m^2) and for the thickest (3 and 4 ML) zinc-blende films. In the latter case, we will see that it is associated with a suppression of the uncompensated polarity. Stabilizing effect of the substrate is much weaker (about 1 J/m^2) in the case of thinner (1 and 2 ML) zinc-blende and in all graphiticlike films.

In oxygen- or magnesium-rich conditions nonstoichiometric films become more stable than the stoichiometric ones. This effect concerns only the thinnest O-rich films (O-Mg-O trilayer) but is systematic in all Mg-rich films. In absence of kinetic effects, one may thus expect that either nonstoichiometric or graphiticlike films will show up in oxidation/growth experiments. We note that the films under consideration display quite different in-plane lattice parameters $a_{\parallel}$. While in the stoichiometric and Mg-rich rocksalt films $a_{\parallel}$ is close to the MgO bulk value of 3.0 Å, it is expanded to about 3.3 Å in the O-rich rocksalt and in zinc-blende films,

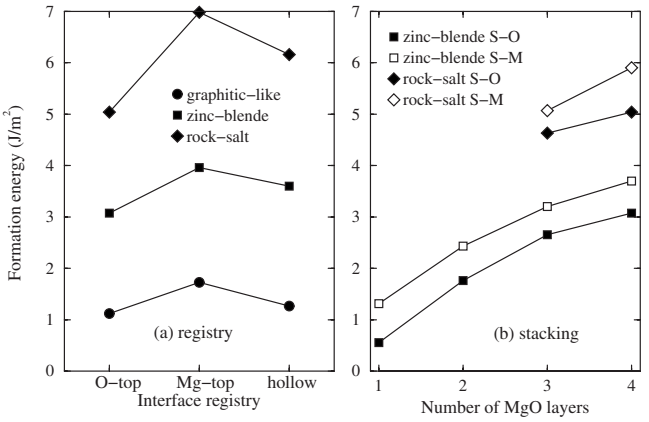

FIG. 2. Formation energies (J/m^2 with respect to bulk MgO) of Pt(111)-supported MgO films in graphiticlike, zinc-blende, and rocksalt structures. (a) Effect of interface registry on 4-ML-thick films with oxygen at the interface: O on-top and Mg hollow (O top), Mg on-top and O hollow (Mg top), and O hollow and Mg hollow (hollow); (b) effect of film stacking: oxygen (S-O) or magnesium (S-M) at the interface.

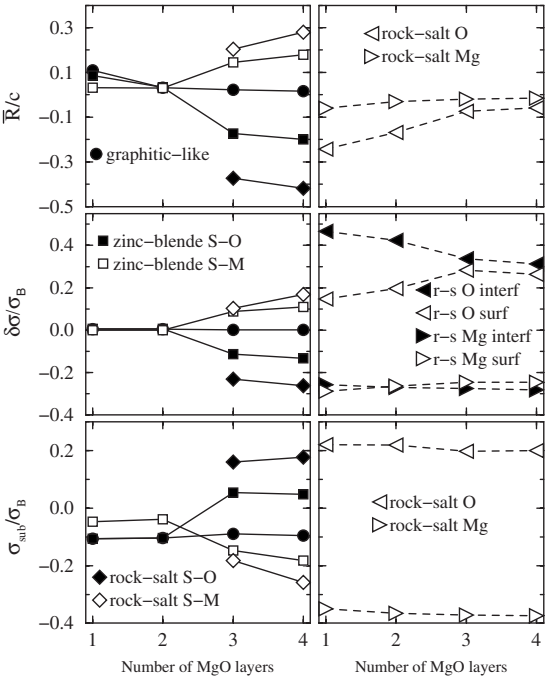

FIG. 3. Normalized average rumpling $\bar{R}/c$, normalized surface charge-density modification $\delta\sigma/\sigma_B$, and normalized substrate charge modification σ_{sub}/σ_B, for stoichiometric (left-hand panel) and nonstoichiometric (right-hand panel), Pt(111)-supported MgO films. In the case of nonstoichiometric films, $\delta\sigma/\sigma_B$ corresponding to the MgO/Pt interface and at the free surface of the oxide film are plotted separately.

and up to about 3.4 Å in the graphiticlike ones.

Figure 2 shows the effect of interface registry and of film stacking on the formation energy of 4-ML stoichiometric MgO films. As far as lattice registry is concerned [Fig. 2(a)], three high-symmetry configurations have been considered: O on-top and Mg hollow (O top), Mg on-top and O hollow (Mg top), and O hollow and Mg hollow (hollow). The results are shown for the most favorable stacking sequence with oxygen layer at the interface. O-top configurations systematically have the lowest energy, while Mg top are the least stable, the energy difference being roughly $1-2$ J/m^2. Stacking effects are shown in Fig. 2(b), for the energetically favored lattice registry: O top for oxygen layers at the interface (S-O stackings) and hollow for magnesium layers at the interface (S-M stackings), respectively.

We find that the stacking does not modify the relative stability of rocksalt and zinc-blende structures. Regardless the precise film structure and thickness, energies of S-O stacking are lower than S-M ones by about $0.5-1.0$ J/m^2. The different nature of the dominant interactions at the interface is responsible for these results: strong O-Pt covalent bonding with a short interface distance and a large charge transfer (O top), as opposed to a weak Mg-Pt bonding with a large interface distance and a small charge transfer (Mg top).

In summary, the interaction with the Pt(111) substrate preserves the relative stability of the three structures found in unsupported films but, in all cases, stabilizes considerably the MgO films. In the following, we will show that the energy lowering is strongly dependent of the polarity characteristics of the oxide film: it is relatively weak for nonpolar films but becomes large for polar-compensated ones and when uncompensated polarity is suppressed. To this goal, in the following section, we will focus more precisely on the polarity-related characteristics of the supported films and on the electrostatic coupling between the surface/interface charge state and the film structure.

IV. MgO/Pt(111): POLARITY CHARACTERISTICS

Figure 3 shows the average film rumpling $\bar{R}/c$, the surface charge-density modification $\delta\sigma/\sigma_B$, and the interfacial charge transfer σ_{sub}/σ_B in Pt(111)-supported MgO ultrathin films. These quantities have been normalized to the distance c between atomic layers of same composition and to the layer charge density σ_B (absolute value) calculated for the corresponding bulk MgO crystals. As before, three structures and two stacking sequences are considered for the stoichiometric films (left panel), and rocksalt structure is considered for the two types of nonstoichiometric ones (right panel).

The average film rumpling $\bar{R}$ is defined as the separation between the centers of gravity of the N_O and N_{Mg} oxygen and magnesium layers, located at elevations z_{iO} and z_{iMg} with respect to the Pt(111) surface

$$\bar{R}/c = \left(\sum_{iO} z_{iO}/N_O - \sum_{iMg} z_{iMg}/N_{Mg} \right)/c.$$

We note that in nonstoichiometric films, a nonzero $\bar{R}/c$ is a measure of film asymmetry with respect to the central atomic layer. The charge-density modification at the free surface of the films

$$\delta\sigma/\sigma_B = \sum_{i \epsilon surface} \delta\sigma_i/\sigma_B$$

is calculated with respect to the corresponding bulk MgO charge values. The summation starts at the free surface and

runs over all layers for which $\delta\sigma_i \neq 0$. At the MgO/metal interface a charge modification occurs both in the oxide film $\delta\sigma_i$ and in the metal substrate $\delta\sigma_{\mathrm{sub}}=\sigma_{\mathrm{sub}}$. Due to the overall charge neutrality, these modifications obey the following relation:

$$\sigma_{\mathrm{sub}}/\sigma_{\mathrm{B}} + \sum_{i\in\mathrm{interface}} \delta\sigma_i/\sigma_{\mathrm{B}} = \begin{cases} -\delta\sigma/\sigma_{\mathrm{B}} & \text{if stoichiometric} \\ \epsilon - \delta\sigma/\sigma_{\mathrm{B}} & \text{if nonstoichiometric} \end{cases}$$

with $\epsilon=1(-1)$ for O (Mg) excess in nonstoichiometric films. With these definitions, polarity compensation in stoichiometric films requires that $\delta\sigma/\sigma_{\mathrm{B}}=\bar{R}/c$. Conversely, nonstoichiometric films with a bulklike rocksalt structure are characterized by $\bar{R}/c\sim 0$ and $\delta\sigma/\sigma_{\mathrm{B}}=+\epsilon/2$.[40]

Figure 3 shows a well-pronounced correlation between the interface charge transfer $\sigma_{\mathrm{sub}}/\sigma_{\mathrm{B}}$, the surface charge state $\delta\sigma/\sigma_{\mathrm{B}}$, and the structure of the oxide film $\bar{R}/c$. In the case of stoichiometric films we note that all graphiticlike and thinner (1–2 ML) zinc-blende films display small (absolute) values of $\bar{R}/c$, $\delta\sigma/\sigma_{\mathrm{B}}$, and $\sigma_{\mathrm{sub}}/\sigma_{\mathrm{B}}$ while these three characteristics are clearly enhanced in thicker (3–4 ML) zinc-blende and in rocksalt films. Positive values of $\bar{R}/c$ are associated to positive $\delta\sigma/\sigma_{\mathrm{B}}$ and negative $\sigma_{\mathrm{sub}}/\sigma_{\mathrm{B}}$, and vice-versa. In nonstoichiometric films, nonzero values of $\bar{R}/c$ in thinnest (1–2 ML) O-rich films correlate with an asymmetry of surface charge state $\delta\sigma/\sigma_{\mathrm{B}}$ between the oxide/metal interface and the free film surface. As a consequence, while polarity compensation is achieved by a substantial modification of the surface charge density $\delta\sigma/\sigma_{\mathrm{B}}$, the polar character of the films can also be deduced from their structure $\bar{R}/c$ or from the behavior of the interface charge transfer $\sigma_{\mathrm{sub}}/\sigma_{\mathrm{B}}$. Figure 3 shows that all considered cases split in two qualitatively different categories.

A. Compensated polarity

On the one hand, thicker (3 and 4 ML) stoichiometric zinc-blende and rocksalt films as well as all nonstoichiometric rocksalt ones, display large values of $\delta\sigma/\sigma_{\mathrm{B}}$ and are polar compensated. As expected from general arguments, $\delta\sigma/\sigma_{\mathrm{B}}$ values are consistent with the calculated $\bar{R}/c$, which witness of a quasibulklike structure of the films. We note that, in all cases, the metal substrate provides the major part of the compensating interfacial charge density. This is similar to the results of our earlier study on constituted metal/MgO(111) interfaces,[33] in which we had shown that the charge compensation by the metal at the interface enables the oxide ions to preserve their valence and stabilizes considerably the polar oxide surface.

Indeed, local density of states (LDOS) plots, Figs. 4 and 5 reveal that, also in supported films, the oxide termination in contact with the metal tends to recover its bulklike characteristics [for unsupported films, see Fig. 3(b) of Ref. 29 and the right panel in Fig. 3 of Ref. 40]. This mechanism determines the sign of the interfacial charge transfer, opposite for

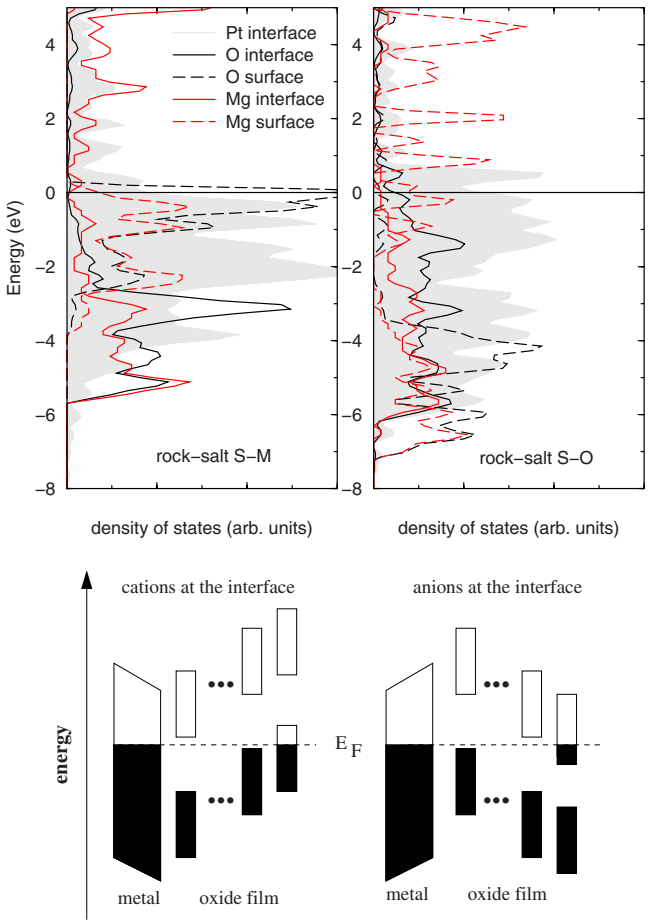

FIG. 4. (Color online) Local density of states of stoichiometric, Pt(111)-supported, 4-ML MgO(111) rocksalt film in the stacking sequences S-O (top-left panel) and S-M (top-right panel). LDOS of interface and surface ions are plotted with, respectively, full and dashed lines. Gray shading is used for LDOS of the Pt substrate. Fermi levels are aligned at the origin of the energy scale. Bottom panels: sketch of the corresponding band alignments.

the two stackings and for the two stoichiometries. Moreover, the metal Fermi level intersects the surface conduction/valence band of the film surface enabling the electron transfer and formation of compensating charge density at the free film surface, as sketched in bottom panels of Figs. 4 and 5. As discussed later, the precise value of σ_{sub} also depends upon metal-oxide bonds which form at the interface.

To summarize, for the films belonging to this category, the electron exchange with the metal substrate is driven by the polar character of the oxide film. It stabilizes the polar compensated state and a bulklike film structure already at small thickness.

B. Substrate-induced polarization

In the case of thinner zinc-blende (1 and 2 ML) and in all graphiticlike (1–4 ML) films, the interfacial charge transfer $\sigma_{\mathrm{sub}}/\sigma_{\mathrm{B}}$ is weak and the average rumpling $\bar{R}/c$ is systematically larger than in their unsupported counterparts. This effect, noticeable at 1 ML, diminishes for thicker films. Con-

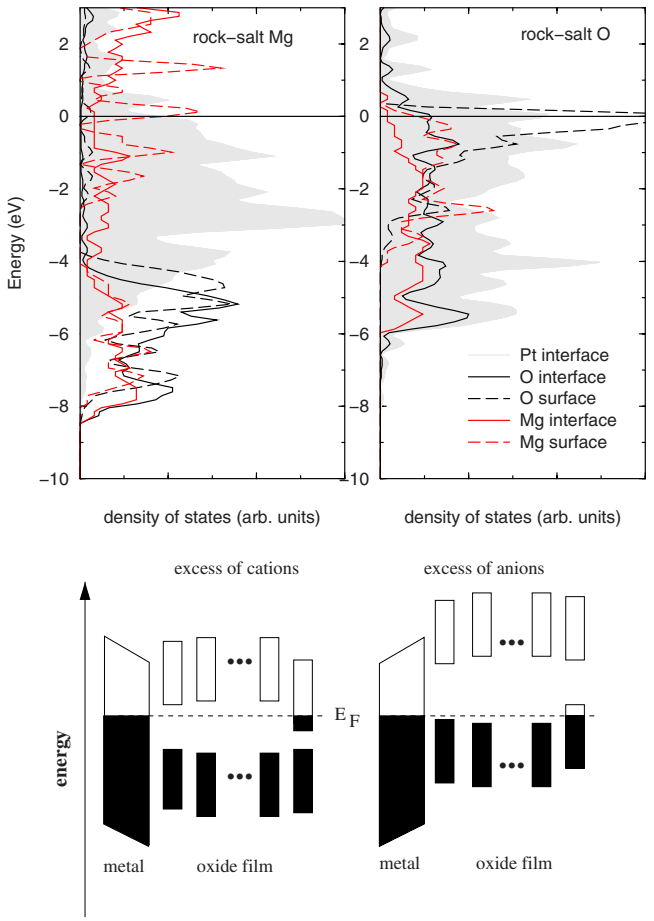

FIG. 5. (Color online) Local density of states of nonstoichiometric, Pt(111)-supported, 4-ML MgO(111) films: Mg rich (left panel) and O rich (right panel). LDOS of interface and surface ions are plotted with, respectively, full and dashed lines. Gray shading is used for LDOS of the Pt substrate. Fermi levels are aligned at the origin of the energy scale. Bottom panels: sketch of the corresponding band alignments.

trary to the compensated polar case described above, electrons are transferred toward the substrate ($\sigma_{sub}/\sigma_B<0$) and oxygen atoms relax outward ($\bar{R}/c>0$) regardless the stacking sequence (zinc-blende films) and the lattice registry (graphiticlike films). In our earlier study on MgO monolayers supported on metal surfaces,[34] we had shown that the electron transfer is driven by the electronegativity of the metal (in the present case the high electronegativity of Pt leads to a negative σ_{sub}) and that the substrate-induced film distortion ($\bar{R}/c>0$) produces a polarization which opposes the dipole moment due to the interfacial electron transfer. The present simulations generalize this scenario and show that the substrate-induced polarization is principally localized at the metal/oxide interface and vanishes rapidly within the oxide film ($\bar{R}/c$ decreases for thicker films). It can be concluded that, in the films belonging to this category, the substrate-induced polarization overrides the either nonpolar (graphiticlike) or uncompensated polar (zinc-blende) character of their unsupported counterparts.

C. Fine substrate-induced effects

Beyond these general features, the formation of stronger Pt-O bonds (as opposed to weaker Pt-Mg ones) at the interface, explains some differences related to stacking or registry. For example, while in all cases σ_{sub} contributes to the compensating charge density at the interface, this contribution is not fully equivalent for the two stacking sequences (stoichiometric films) or for the two stoichiometries. Indeed, electron transfer toward the metal substrate (negative σ_{sub}) is systematically larger than that toward the oxide film (positive σ_{sub}). We have noted the same trend in the analysis of metal/MgO interfaces,[33] and associated it to the formation of interfacial bonds and to the high electronegativity of Pt.

In addition, in stoichiometric rocksalt films, while $\bar{R}/c$ and $\delta\sigma/\sigma_B$ are quasibulklike for S-O stacking, they are by nearly 50% smaller in the case of S-M stacking. This latter effect can be attributed to the relatively strong O-Pt interaction at the interface (short O-Pt distance) which, in conjunction with a weak Mg-Pt interaction (long Mg-Pt distance), results in an effective flattening of the films.

Finally, in the thinnest (1 and 2 ML) oxygen-rich rocksalt films, the symmetry of both structural and electronic characteristics with respect to the central atomic layer, present in unsupported films, is broken. We find $\bar{R}/c\neq 0$ and a different charge state at the free surface and at the interface. The effect is driven by a structural distortion due to a strong Pt-O interaction at the interface which shifts the center of gravity of oxygen layers toward the interface, $\bar{R}/c<0$. The dipole moment due to this structural distortion is opposed and partially compensated by the one due to the charge redistribution between the two film terminations. As a consequence, the (absolute) value of the charge state at the interface is larger than that at the free surface.

In summary, we have shown that the electron exchange between the metal substrate and the oxide film is at the origin of two different effects. On one hand, it contributes to the polarity compensation at the interface and enhances considerably the stability of the compensated polar films. On the other hand, it induces structural distortions of the films in the interface region which either polarize the nonpolar films or override the polarization of the uncompensated polar ones.

V. MgO/Pt(111): DIPOLE MOMENT AND WORK FUNCTION

In this section we focus on the total dipole moment of the supported oxide films, a quantity which represents the modification of the work function of the metal substrate, and which determines the surface characteristics of the constituted oxide/metal support. Figure 6 shows that the oxide layer gives a substantial contribution to the total work function, which can either increase (positive dipole values) or reduce (negative dipole values) that of the bare metal surface. We note that the total dipole moments, and, in particular, their sign, are correlated with the surface charge state $\delta\sigma/\sigma_B$, Fig. 3, and thus to the polarity characteristics of the oxide films. However, an important negative contribution comes from the compression of the electronic density at the

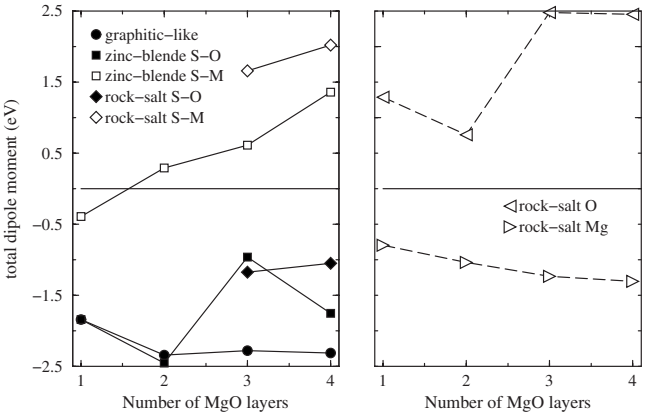

FIG. 6. Total dipole moment (eV) of Pt(111)-supported MgO stoichiometric films for two stacking sequences (S-O and S-M) (left panel) and for nonstoichiometric Mg- and O-rich rocksalt films (right panel).

metal/oxide interface, which systematically lowers the total work functions,[10,41] and drives the behavior of the total dipole moment in the case of graphiticlike and thinner (1–2 ML) zinc-blende films.

Indeed, in the case of compensated polar films (stoichiometric 3–4-ML zinc bende and rocksalt, nonstoichiometric 1–4-ML rocksalt), the dipole moment is mainly determined by the mechanism which drives the surface charge state $\delta\sigma/\sigma_B$. In stoichiometric films with S-M (S-O) stacking sequence, its main positive (negative) component is due to the residual dipole across the oxide film, necessary to shift the metal Fermi level E_F below the valence-band maximum (VBM) [above the conduction-band minimum (CBM)] of the free film surface, see Fig. 4. Neglecting bandwidth effects, it can be estimated as $D_{S\text{-}M} \sim E_F - \text{VBM}$ and $D_{S\text{-}O} \sim E_F - \text{CBM}$. This is consistent with $-D_{S\text{-}O} \sim D_{S\text{-}M}$ in zinc-blende films, where the metal Fermi level is approximately located in the center of the gap, and $-D_{S\text{-}O} < D_{S\text{-}M}$ in rocksalt films, where the metal Fermi level is in the upper half of the band gap. We note that $D_{S\text{-}M} - D_{S\text{-}O}$ is on the order of the oxide bandwidth (and actually somewhat smaller due to the neglect of bandwidth effects). Conversely, in nonstoichiometric films (zero dipole moment when unsupported), the sign and the strength of the dipole moment is determined by the interface charge transfer σ_{sub}, Fig. 3. While these arguments explain the main characteristics of the total dipole moments as a function of film stacking and stoichiometry, the precise values are also dependent on the bonding characteristics at the interface.

At variance, in films which are only polarized by the metal substrate, the main component of the total dipole moment is negative and due to the combined effect of the electron-density compression at the interface (always negative) and of the interfacial charge transfer (negative due to $\sigma_{sub} < 0$). In 1-ML-thick graphiticlike and zinc-blende films, the latter (negative) component is partially compensated by the positive dipole moment due to the film rumpling $\bar{R}/c > 0$ (see above). In 2-ML zinc-blende films in S-M stacking, the combined negative component is overridden by the intrinsic positive dipole due to the S-M stacking.

While the relative weights of different contributions vary, we note that all supported MgO films produce total dipole moments of a similar magnitude (see, e.g., the three stoichiometric films in the preferential, S-O stacking). As a consequence, change of the work function on its own can hardly be considered as an unambiguous signature of polar character.

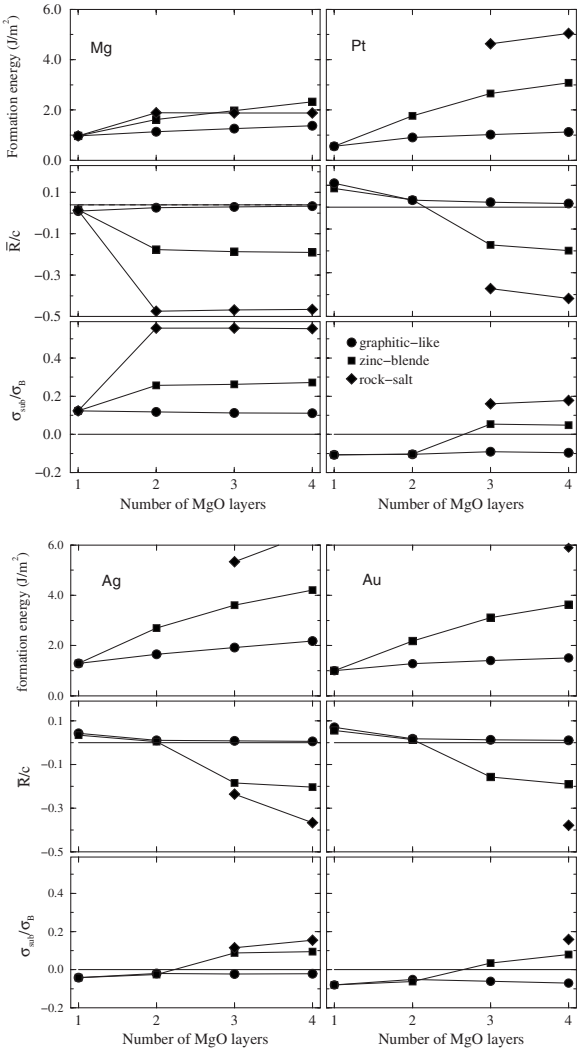

FIG. 7. Formation energy with respect to bulk MgO (J/m^2), normalized average rumpling $\bar{R}/c$, and normalized charge density of the metal substrate σ_{sub}/σ_B, for stoichiometric MgO films supported on Mg(0001), Pt(111), Ag(111), and Au(111) surfaces, with graphiticlike, zinc-blende, and rocksalt structures.

VI. SYSTEMATICS AS A FUNCTION OF METAL SUBSTRATES

In order to determine to which extent the mechanisms analyzed above in the particular case of MgO/Pt(111) are generic and relevant for other metal substrates, we consider MgO films supported on a series of metals ranging from simple (Mg), to transition (Pt), and noble (Ag, Au).

Figure 7 summarizes the energetic, structural, and electronic characteristics of supported MgO films: the formation energy, the normalized average rumpling $\bar{R}/c$, and the normalized charge density of the metal substrate σ_{sub}/σ_B. We

have already reported these characteristics in the case of the Pt(111) substrate (see Sec. III, Fig. 1 and Sec. IV, Fig. 3) and discussed the mechanisms underlying their behavior. Comparison of these data for the series of metals enables a discussion of the effect of substrate electronegativity (in particular, contrary to considered transition and noble metals, low electronegativity of Mg privileges an electron transfer toward the MgO film[34]) and of the strength of metal-oxygen bonds at the interface (particularly weak in the case of Ag).

Figure 7 shows that the general trends discussed in the case of Pt hold also for other substrates. On one hand, metal substrates systematically stabilize the oxide films, the effect being particularly well pronounced for the polar compensated ones. We note that polarity compensation is the most efficient at the Mg substrate, leading to the least pronounced energy differences for of the three structures under consideration. Moreover, stoichiometric rocksalt films on Mg(0001) are metastable also at the smallest thickness, and both rocksalt and zinc-blende films show bulklike structural characteristics starting already 2 ML (see the corresponding bulklike values of $\bar{R}/c$).

On the other hand, similarly to the case of Pt substrate discussed in Sec. III, we find the systematic relationship between film structural characteristics $\bar{R}/c$ and the interface charge transfer σ_{sub}/σ_B, the latter being correlated to the oxide surface charge state, $\sigma_{sub}/\sigma_B \sim -\delta\sigma/\sigma_B$. As a consequence, the two categories of behavior discussed in Sec. III can also be identified at other substrates. Indeed, in all cases of polar compensated films (rocksalt films: 2–4 ML on Mg, 3–4 ML on Ag and Pt, 4 ML on Au and zinc-blende films: 2–4 ML on Mg, 3–4 ML on Ag, Pt, and Au), regardless the metal electronegativity, the interface charge transfer $\sigma_{sub}/\sigma_B \sim -\bar{R}/c$ is principally driven by the polar character of the film, its positive sign being systematically determined by the preferential S-O stacking at the oxide/metal interface.

Conversely, in the case of nonpolar or uncompensated polar films (graphiticlike films: 1–4 ML on Mg, Ag, Pt, and Au and zinc-blende films: 1 ML on Mg, 1–2 ML on Ag, Pt, and Au), the metal substrates induce a nonvanishing polarization. While the average rumpling remains correlated with the interface charge transfer $-\bar{R}/c \sim \sigma_{sub}/\sigma_B$, the latter is driven by the electronegativity of the metal substrate, rather than by the structure of the oxide film. Indeed, charge transfer toward the oxide ($\sigma_{sub}>0$) is favored on Mg (low electronegativity) while electrons are transferred toward the metal ($\sigma_{sub}<0$) at substrates of higher electronegativity (Pt, Ag, and Au).

Our results show that, while the interface charge transfer induced by the polarity of the oxide film is systematically larger than the one driven by the substrate electronegativity, the latter is present at both polar and nonpolar metal/oxide interfaces. As a consequence, depending on the precise oxide/metal system, the two contributions to the interface charge transfer may either act along (MgO/Mg) or oppose each other (MgO/Ag, MgO/Pt, and MgO/Au). In this context, the enhanced stabilizing effect of the Mg substrate can be seen as due to its low electronegativity and to the resulting synergy between the two mechanisms of charge transfer at the MgO/Mg interface. Conversely, higher electronegativity of Ag, Pt, and Au favors $\sigma_{sub}<0$, which opposes the polarity compensation requirement for the preferential S-O stacking ($\sigma_{sub}>0$).

Finally, similarly to the case of the Pt(111) substrate, also for the other metals different film structures are characterized by considerably different values of in plane lattice parameter $a_{\parallel}$. While one has to keep in mind the approximate character of our present estimation of $a_{\parallel}$, it may provide a guideline for the structural characterization of MgO films grown experimentally. Indeed, the considerably expanded in-plane lattice parameter of 3.25 Å (2 ML) and 3.28 Å (10 ML), measured for planar (1×1) MgO(111) films on Ag(111),[22,23] seems incompatible with the calculated stoichiometric rocksalt structure ($a_{\parallel}$=3.2 and 3.1 Å, respectively, for 3 and 4 ML), and points toward the zinc blende ($a_{\parallel}\sim3.3$ Å for both 3 and 4 ML) or the graphiticlike structure ($a_{\parallel}\sim3.45$ Å), both of them being considerably more stable energetically, Fig. 7. On the other hand, lattice parameters close to the bulk MgO value, derived from experiments on MgO(111)/Ag(111) (Ref. 25) and MgO(111)/Au(111) (Ref. 27) are consistent with the supported rocksalt films and may thus suggest a possibility of nonstoichiometry and/or of surface hydroxylation.

VII. CONCLUSIONS

In summary, to identify generic mechanisms of interaction between polar oxide films and a metal substrate we have performed DFT calculations on ultrathin polar MgO(111) films of different structures, layer stacking and lattice registry at the interface, deposited on a series of different metal substrates (Mg, Pt, Ag, and Au). We have shown that the substrate provides charges participating to polarity compensation: an electron transfer, which screens the compensating charges at the interface and which allows the interfacial oxide ions to recover their usual valence, takes place across the metal/oxide interface. This induces a strong stabilization of polar films. In addition, due to bond formation at the interface and to band alignment, a second type of electron exchange occurs at the interface, driven principally by the electronegativity of the metal substrate. In nonpolar or uncompensated polar films, this charge transfer induces a structural distortion of the oxide film in the interface region and a polarization which contributes to the modification of the substrate work function. In the case of polar compensated films, the present results suggest the possibility of an extensive tuning of the surface work function of the composite metal/oxide support by changes in the film structure (stacking sequence) and stoichiometry.

ACKNOWLEDGMENTS

We thank N. Nilius and G. Pacchioni for stimulating discussions. We acknowledge support from the COST Action D41 *Inorganic oxides: surfaces and interfaces* and from the French ANR *SIMINOX* under Project No. ANR-06-NANO-009-01.

[1] L. Savio, E. Celasco, L. Vattuone, and M. Rocca, J. Chem. Phys. **119**, 12053 (2003).
[2] S. Altieri, S. F. Contri, and S. Valeri, Phys. Rev. B **76**, 205413 (2007).
[3] A. M. Ferrari, C. Roetti, and C. Pisani, Phys. Chem. Chem. Phys. **9**, 2350 (2007).
[4] Y.-N. Sun, Z.-H. Qin, M. Lewandowski, E. Carrasco, M. Sterrer, S. Shaikhutdinov, and H.-J. Freund, J. Catal. **266**, 359 (2009).
[5] A. Hellman, S. Klacar, and H. Gronbeck, J. Am. Chem. Soc. **131**, 16636 (2009).
[6] Y.-N. Sun, L. Giordano, J. Goniakowski, M. Lewandowski, Z.-H. Qin, C. Noguera, S. Shaikhutdinov, G. Pacchioni, and H.-J. Freund, Angew. Chem. Int. Ed. (to be published).
[7] D. Ricci, A. Bongiorno, G. Pacchioni, and U. Landman, Phys. Rev. Lett. **97**, 036106 (2006).
[8] M. Sterrer, T. Risse, M. Heyde, H.-P. Rust, and H.-J. Freund, Phys. Rev. Lett. **98**, 206103 (2007).
[9] L. Giordano, J. Goniakowski, and G. Pacchioni, Phys. Rev. B **67**, 045410 (2003).
[10] L. Giordano, F. Cinquini, and G. Pacchioni, Phys. Rev. B **73**, 045414 (2006).
[11] U. Martinez, L. Giordano, and G. Pacchioni, J. Chem. Phys. **128**, 164707 (2008).
[12] F. Cinquini, L. Giordano, G. Pacchioni, A. M. Ferrari, C. Pisani, and C. Roetti, Phys. Rev. B **74**, 165403 (2006).
[13] F. E. Olsson and M. Persson, Surf. Sci. **540**, 172 (2003).
[14] L. Giordano, G. Pacchioni, J. Goniakowski, N. Nilius, E. D. L. Rienks, and H.-J. Freund, Phys. Rev. B **76**, 075416 (2007).
[15] G. Pacchioni, L. Giordano, and M. Baistrocchi, Phys. Rev. Lett. **94**, 226104 (2005).
[16] L. Giordano and G. Pacchioni, Phys. Chem. Chem. Phys. **8**, 3335 (2006).
[17] P. Frondelius, H. Hakkinen, and K. Honkala, New J. Phys. **9**, 339 (2007).
[18] L. Giordano, G. Pacchioni, J. Goniakowski, N. Nilius, E. D. L. Rienks, and H.-J. Freund, Phys. Rev. Lett. **101**, 026102 (2008).
[19] M. Sterrer, T. Risse, U. M. Pozzoni, L. Giordano, M. Heyde, H.-P. Rust, G. Pacchioni, and H.-J. Freund, Phys. Rev. Lett. **98**, 096107 (2007).
[20] N. Nilius, E. D. L. Rienks, H.-P. Rust, and H.-J. Freund, Phys. Rev. Lett. **95**, 066101 (2005).
[21] N. Berdunov, G. Mariotto, K. Balakrishnan, S. Murphy, and I. V. Shvets, Surf. Sci. Lett. **600**, L287 (2006).
[22] M. Kiguchi, S. Entani, K. Saiki, T. Goto, and A. Koma, Phys. Rev. B **68**, 115402 (2003).
[23] R. Arita, Y. Tanida, S. Entani, M. Kiguchi, K. Saiki, and H. Aoki, Phys. Rev. B **69**, 235423 (2004).
[24] S. Entani, M. Kiguchi, and K. Saiki, Surf. Sci. **566-568**, 165 (2004).
[25] M. Mantilla, N. Jedrecy, R. Lazzari, and J. Jupille, Surf. Sci. **602**, 3089 (2008).
[26] M. Xue and Q. Guo, J. Chem. Phys. **127**, 054705 (2007).
[27] P. Myrach, S. Benedetti, S. Valeri, N. Nilius, and H.-J. Freund (unpublished).
[28] J. Goniakowski, C. Noguera, and L. Giordano, Phys. Rev. Lett. **93**, 215702 (2004).
[29] J. Goniakowski, C. Noguera, and L. Giordano, Phys. Rev. Lett. **98**, 205701 (2007).
[30] C. Noguera, J. Phys.: Condens. Matter **12**, R367 (2000).
[31] J. Goniakowski, F. Finocchi, and C. Noguera, Rep. Prog. Phys. **71**, 016501 (2008).
[32] J. Goniakowski and C. Noguera, Phys. Rev. B **60**, 16120 (1999).
[33] J. Goniakowski and C. Noguera, Phys. Rev. B **66**, 085417 (2002).
[34] J. Goniakowski and C. Noguera, Phys. Rev. B **79**, 155433 (2009).
[35] J. P. Perdew and Y. Wang, Phys. Rev. B **45**, 13244 (1992).
[36] D. Vanderbilt, Phys. Rev. B **41**, 7892 (1990).
[37] G. Kresse and J. Hafner, Phys. Rev. B **47**, 558 (1993); G. Kresse and J. Furthmüller, *ibid.* **54**, 11169 (1996).
[38] R. F. W. Bader, Chem. Rev. **91**, 893 (1991).
[39] G. Henkelman, A. Arnaldsson, and H. Jonsson, Comput. Mater. Sci. **36**, 354 (2006); W. Tang, E. Sanville, and G. Henkelman, J. Phys.: Condens. Matter **21**, 084204 (2009).
[40] C. Noguera and J. Goniakowski, J. Phys.: Condens. Matter **20**, 264003 (2008).
[41] J. Goniakowski and C. Noguera, Interface Sci. **12**, 93 (2004).